

## Article

# Choice of the Arch Yielding Support for the Preparatory Roadway Located near the Fault

Krzysztof Skrzypkowski <sup>1,\*</sup>, Krzysztof Zagórski <sup>2</sup>, Anna Zagórska <sup>3</sup>, Derek B. Apel <sup>4</sup>, Jun Wang <sup>4</sup>, Huawei Xu <sup>4</sup> and Lijie Guo <sup>5,6</sup>

- <sup>1</sup> Faculty of Civil Engineering and Resource Management, AGH University of Science and Technology, Mickiewiczza 30 Av., 30-059 Kraków, Poland
- <sup>2</sup> Faculty of Mechanical Engineering and Robotics, AGH University of Science and Technology, Mickiewiczza 30 Av., 30-059 Kraków, Poland; zagkrzys@agh.edu.pl
- <sup>3</sup> Research Centre in Kraków, Institute of Geological Sciences, Polish Academy of Science, Senacka 1, 31-002 Kraków, Poland; ndzagors@cyf-kr.edu.pl
- <sup>4</sup> School of Mining and Petroleum Engineering, University of Alberta, Edmonton, AB T6G 2R3, Canada; dapel@ualberta.ca (D.B.A.); jun8@ualberta.ca (J.W.); hx1@ualberta.ca (H.X.)
- <sup>5</sup> BGRIMM Technology Group, No. 22, Beixing Road, Daxing District, Beijing 102628, China; guolijie@bgrimm.com
- <sup>6</sup> National Centre for International Research on Green Metal Mining, Beijing 100160, China
- \* Correspondence: skrzypko@agh.edu.pl

**Abstract:** The article presents a method of selecting an arch yielding support for preparatory workings driven in a hard coal seam. Particular attention was paid to discontinuous deformation in the form of a fault, which significantly contributes to the change of the excavation protection schemes. On the basis of the geometry of the machines and devices in the designed excavation, the support was selected, which was then checked for the ventilation criterion. In the next stage, analytical calculations were carried out using the determined spacing of the steel support in the fault zone and the area outside of it. Additionally, using the RS3 numerical software based on the finite element method, a rock mass model with a fault was built, through which the preparatory excavation passes. The aim of the research was to determine the total displacements occurring in the fault crossing zone for the excavation without support and with the use of steel arch yielding and with additional reinforcement in the form of straight segments. In conclusion, it was found that the variants of the excavation reinforcement can be modeled and selected in advance, which allows for the fastest possible execution of the driving and the maintenance of the minimum movement dimensions while passing through the fault.

**Keywords:** arch yielding support; fault; minimal section method; RS3



**Citation:** Skrzypkowski, K.; Zagórski, K.; Zagórska, A.; Apel, D.B.; Wang, J.; Xu, H.; Guo, L. Choice of the Arch Yielding Support for the Preparatory Roadway Located near the Fault. *Energies* **2022**, *15*, 3774. <https://doi.org/10.3390/en15103774>

Academic Editor: Sergey Zhironkin

Received: 24 April 2022

Accepted: 19 May 2022

Published: 20 May 2022

**Publisher's Note:** MDPI stays neutral with regard to jurisdictional claims in published maps and institutional affiliations.



**Copyright:** © 2022 by the authors. Licensee MDPI, Basel, Switzerland. This article is an open access article distributed under the terms and conditions of the Creative Commons Attribution (CC BY) license (<https://creativecommons.org/licenses/by/4.0/>).

## 1. Introduction

Underground mining of hard coal deposits requires the construction and maintenance of many preparatory workings, which are driven by a certain time advance in relation to the exploitation of the deposit. Such a technological process makes it necessary to ensure the stability of workings in the long term. These issues are of particular importance in relation to preparatory workings, the useful life of which is often related to the life of longwalls. Preparatory workings are located in an environment with many geological factors, such as continuous and discontinuous deformations, high stresses and natural hazards [1], including the impact of remains and operating edges [2] that contribute to additional loads on mining supports. Both the roadways and inclined drifts are supported by an independent arch yielding support [3]; rock bolt and cable support [4–6], including steel arch and bolts [7,8]; and shotcrete [9,10], or new solutions are sought with the use of a hydraulic support [11]. The previously used steel sets support is often exposed to the influence of saline mine waters [12]. First of all, leaks occur in different places and

periods of the excavation's existence, depending on the degree of fracture and crushed rocks in the fault area [13,14]. Driven preparatory excavations in the immediate vicinity of the fault are secured with a support, the main task of which is to ensure the stability of the excavation throughout its lifetime and the dimensions of its cross-section, as well as to protect people, machines and devices against rock fragments moving from the roof or side walls [15]. In conditions of additional loads caused by the immediate vicinity of the fault, the arch yielding support should be characterized by a defined load capacity resulting from the strength parameters of its individual elements and the ability to deform under control [16]. The occurrence of changes in the geometry of the support without damaging its structural elements is ensured by the appropriate flexibility of the support as well as its spacing. The individual arches of the steel support, set at specific intervals, are connected with each other by means of struts that keep the distance between them and prevent them from twisting in the event of uneven loading. The length of the struts is usually adjusted to the spacing of the arches with a pitch of at least 0.1 m. Most often, this pitch is 0.25 m, which translates into the distance between the frames: 0.5, 0.75, 1.0, 1.25, 1.5 m [17]. The flexibility of the support provides the possibility of displacement of the support structural elements in relation to each other as a result of the impact of specific load values. The selection of the arch yielding support of the preparatory workings is made with the assumption of the safety coefficients [18]. The basic factor determining the stability of the excavation is the correct selection of the parameters of the support, both in terms of geometry and strength. This selection is based on the assumption that the designed excavation is made in rocks with specific strength, deformation and structural parameters. The mutual relation of these values determines the processes taking place in the vicinity of the excavation exposed to the fault and directly determines the spacing of the support. Important factors influencing the load-bearing capacity of the arch yielding support include the physical and mechanical parameters of the steel used to make individual elements of the support of mining excavations [19]. Currently, the most commonly used steel grades are 25G2, 34GJ, 31Mn4, S480W, G480V, S550W and HL CORR, which are characterized by their yield point and minimum tensile strength of 340 MPa and 550 MPa, respectively [20]. The need to verify theoretical solutions has led to the creation and development of laboratory stands in research and development units, the task of which is to better understand the behavior of the structure [21] and the cooperation of the support with the rock mass [22]. Yang et al. [23] pointed out top and bottom arch strengthening for a new steel sets designed for underground roadways. Lv et al. [24] conducted laboratory test of square steel confined concrete in a geometric scale 1:1 and indicated the possible places of damage. Wu et al. [25] simulated the surrounding rock stress by means of the model tests. As a result of the recognition of the impact of various physicommechanical factors, it is possible to make a practical assessment of the application of the steel sets in natural conditions. Research on physical models, which reflect the impact of the fault on the stability of the excavation, is of particular importance. Wang et al. [26] stated that the presence of fault increases the risk of dynamic phenomena. Wang et al. [27] pointed out that in the immediate vicinity of the fault, there is a great risk of sudden rock fall into the excavation. A common method of reinforcing the excavation while passing through the fault is the use of an additional bolt and cable support [28]. Adoko et al. [29] used RS2 software to model drift with and without supports. According to their calculations, the use of rock bolting and concrete contributed to a more than two-fold reduction in the value of stresses around the excavation. Xiong et al. [30] found and proved on the basis of numerical modeling that the combination of several types of support contributes to an effective and significant reduction in roadway deformation, thanks to which the excavation retains its functionality for longer. The irregularities in the deposits of hard coal can be divided into primary and secondary. The primary irregularities arose simultaneously with seam formation and secondary irregularities after the seam formation. For the selection of the casing and operation, the greatest challenge includes faults (Figure 1a), which are the shifts of the layers in relation to each other with a simultaneous interruption of their continuity. The shifts occur along the cracks in the

rock mass. In the case of a normal fault, the fault plane is inclined towards the dropped wing. On the other hand, for an inverted fault, the layer overlap occurs in such a way that the older layers lie partially over the younger ones. Depending on the direction of the fault plane in relation to the seam strike, longitudinal faults (Figure 1b) and transverse faults (Figure 1c) are distinguished. The fault is longitudinal when the contours of the step plane run parallel to the extent of the seam, transverse when the contours run perpendicular to the extent. In addition, there are also oblique faults where the contours of the fault plane form a right angle with the length of the deck. The gap along which the layers have shifted is called the fault gap. Fault fissures are often water-bearing and constitute one of the sources of water inflow to underground mine's workings. In hard coal seams, faults are sometimes reservoirs of gases, such as carbon dioxide or methane. Sometimes, the disturbed layers adhere tightly to each other in a plane smoothly polished by rock friction while moving. The wider fault gaps are filled with rock crumbs, sand and clay.

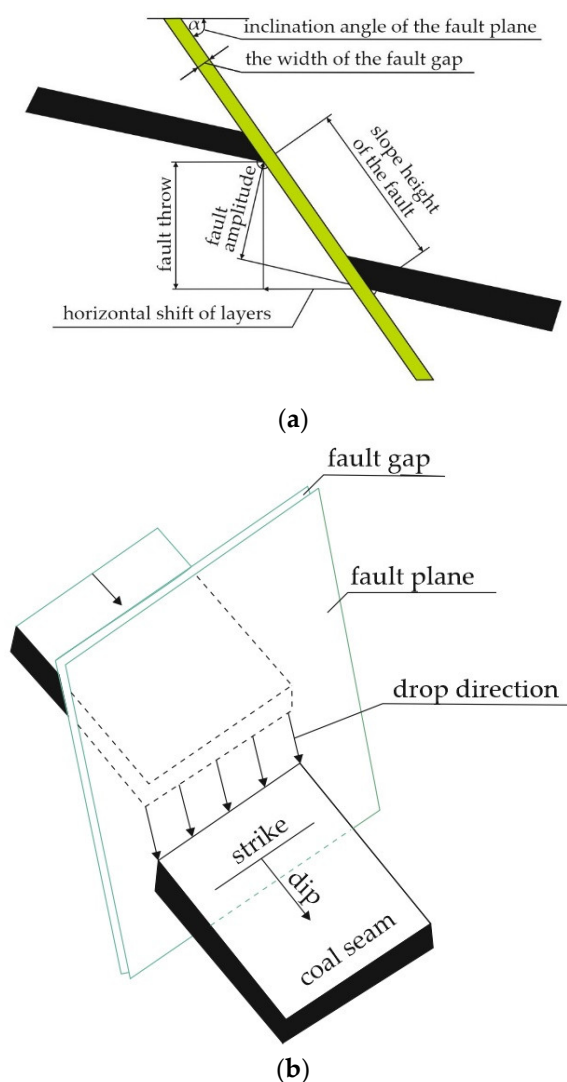


Figure 1. Cont.

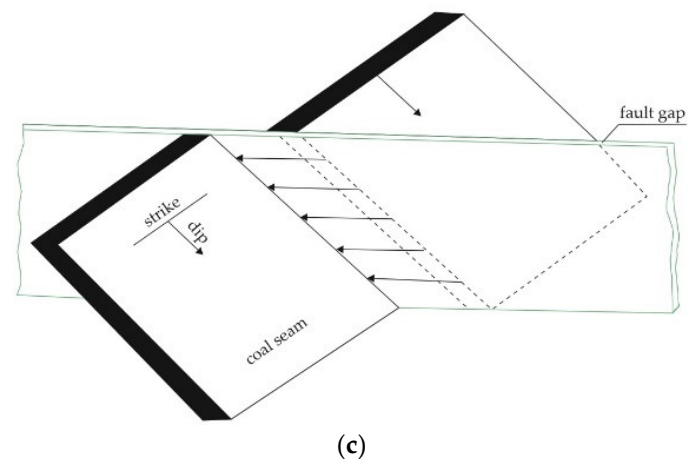


Figure 1. Fault: (a) basic parameters; (b) longitudinal; (c) transverse.

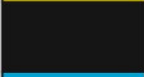
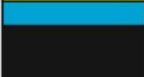
Despite significant progress in the selection of the arch yielding support for underground preparatory workings and numerous laboratory, numerical and industrial tests, there is still a gap in the calculation algorithm in taking into account the selection of fore-head equipment, ventilation criterion and geomechanical calculations. The article presents a method of selecting the arch yielding support for the preparatory excavation, which was driven in the fault zone. Based on analytical calculations, the support spacing in the immediate fault zone as well as outside of it was calculated. Using the spatial numerical software based on the finite element method, three variants of the excavation performance were modeled: without support; with the use of steel arch yielding; and with additional reinforcement in the form of straight segments. The results of the numerical simulations were the total displacement distributions around the driven preparatory roadway.

## 2. Mining and Geological Conditions of the Driven Excavation

Rock lumps of hard coal, claystone and sandstone were collected from the 800 m level roadway in one of the mines of the Upper Silesian Coal Basin in Poland. The forehead is driven mechanically with the R-130 roadheader (Figure 2), while the excavated material from the face is loaded with the machine loader onto the belt feeder. The extent of geological layers in the area of the planned works generally runs along NNW–SEZ. The collapse of the layers does not exceed  $3^\circ$ , generally NE. The excavation is driven in the layer of coal seam 207 with a thickness of about 4 m. Directly at the roof and the floor of the excavation, there is a layer of claystone over which there is a several dozen meter layer of sandstone (Figure 3).



Figure 2. Forehead, place of sampling.

Column	Description	Range of thickness variations, (m)
	sandstone	10–30
	coal seam 206	1.3–2.8
	claystone	0.4–2.0
	coal seam 206	0.1–0.5
	claystone	0.1–4.5
	sandstone	19–28
	claystone	0.1–0.9
	coal seam 207	2.5–4.1
	claystone	0.1–2.8
	sandstone	13–57

**Figure 3.** Lithological profile of the coal seam.

The roadway is driven in a rock mass where there is no methane hazard, and above all, it is made outside the area that is subject to rock bursts and gas and rock outbursts. The excavation is classified as “A” class of coal dust explosion hazard, which means that in the driven coal seam or its part, there is mine dust protected in a natural way. In addition, mine dust contains at least 80% of non-flammable solids of natural origin, the amount of hazardous coal dust is less than  $10 \text{ g/m}^3$  of the excavation and the mass of coal dust without non-flammable solids, settling on a given surface at a given time hereinafter referred to as dust settling intensity, is less than  $0.15 \text{ g/m}^2$  per day [31]. Coal seam no. 207 was classified into the fifth most dangerous group of self-igniting. The incubation period of endogenous fire is 32 days, while the activation energy  $A$  is  $46.5 \text{ kJ/mol}$ , and the self-igniting index  $S_{za}$  is  $137 \text{ }^\circ\text{C/min}$  [32]. In the vicinity of the designed excavation, the temperature of rocks is about  $20 \text{ }^\circ\text{C}$ . The conducted measurements and their results as well as the practice acquired during the exploitation of the coal seam no. 207 indicate that, during driving, the substitute climate temperature should not exceed  $26 \text{ }^\circ\text{C}$  for workplaces. In the event of a water hazard, the excavation area was classified as the weakest in a three-point scale. Water to the preparatory roadway can flow mainly from the depletion of carboniferous aquifers associated with sandstones lying between seams 206 and 207 in the form of condensation and roof leakages. In the area of the excavation, there is a geological disturbance in the form of faults with a throw size from 1.8 m to 2.5 m, which occurred along the north–eastern side of the side (Figure 4).



**Figure 4.** The area of the roadway with marked faults.

#### *Laboratory Tests of Rocks from Driven Excavation*

In the laboratory of the Department of Mining Engineering and Occupational Safety of AGH in Krakow, cylindrical samples with a diameter of 50 mm and a height of 100 mm were cut using a core drill (Figure 5a,b). The samples prepared in this way were tested (Figure 5c–e) on a testing machine, which was equipped with three strain gauges and a cable encoder to measure the displacement, while the horizontal strains were measured with three electronic dial gauges (Figure 5c). The load rate was 0.5 kN/s. The results are summarized in Table 1. The main objective of the laboratory tests was to determine the deformation and strength parameters of three types of rocks, coal, sandstone and clay slate, which surround the hard coal seam. In the laboratory tests, no rheological tests of hard coal related to creep and relaxation were performed, because the hard coal showed the characteristics of an elastic-brittle material. The test results were used in numerical modeling to estimate the total displacement for different variants of roadway II protection. All types of rock were taken from the forehead of the roadway II. There was no visible stratification in the rocks from which samples of both coal, sandstone and clay slate had been cut.

**Table 1.** Summary of the results of strength and deformation tests for rocks in the area of the designed excavation.

Type of Rock	Density (kg/m <sup>3</sup> )	Compressive Strength (MPa)	Tensile Strength (MPa)	Young's Modulus (GPa)
Coal	1296	15.45	1.37	2.3
Claystone	2440	16.5	1.55	10.3
Sandstone	2560	47	3.62	5.4

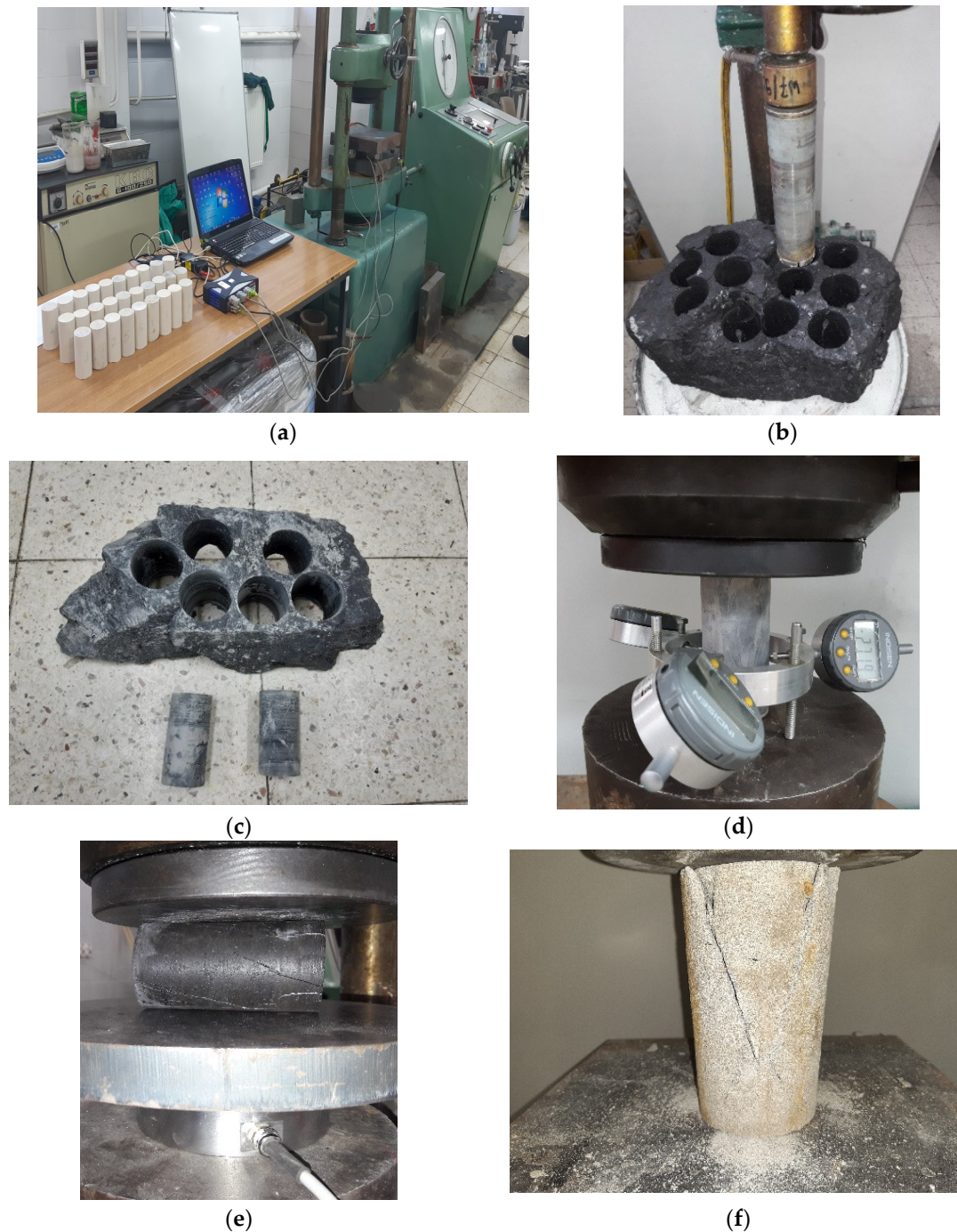


**Figure 5.** Preparation of samples for testing: (a) testing machine equipped with sensors; (b) cutting samples in a block of coal with a trepan drill; (c) a lump of clay slate with samples cut out; (d) electronic sensors of horizontal deformation; (e) Brazilian tensile strength test; (f) compression of sandstone samples.

### 3. Choice of the Arch Yielding Support

#### 3.1. Minimum Section Method

In order to determine the dimensions of the cross-section of roadway II, the method of minimum sections was first used, which consists in determining the minimum width and minimum height of the excavation. In order to determine the minimum width  $S_{\min}$ , all widths of devices in the excavation and the minimum movement distances between the devices and the excavation support were added [33]. The minimum height  $H_{\min}$  is

calculated as the minimum height, but the dimensions are summed up in the largest cross-section. The sum of the width and height together with the movement distances should be multiplied by 1.1 due to the possibility of clamping the excavation, thus reducing the excavation cross-section. The individual widths and heights of machines and devices along with the minimum movement distances are presented in Table 2.

**Table 2.** Dimensions of machines and devices with minimum movement distances.

Type of Machine or Device	Width (mm)	Height (mm)
Suspended monorail: BIZON 120-X	1200	1500
Belt conveyor: GWAREK-1000	1350	1000
Fire pipeline	315	
Drainage pipeline	315	
Compressed air pipeline	250	
Duct diameter	1000	
Passage for miners	700	1800
Rail of suspended monorail	155	
Movement intervals		
From	To	Minimum distance (mm)
Belt conveyor	Arch yielding support	250
Suspended monorail	Belt conveyor	400
Duct	Belt conveyor	600
Floor	Suspended monorail	300
Rail of suspended monorail	Roof arch	500

The minimum width  $S_{\min}$  and the height  $H_{\min}$  of the excavation were determined according to Equations (1) and (2):

$$S_{\min} = \left( \sum x_a + \sum x_b \right) \cdot 1.1 \text{ (mm)}, \quad (1)$$

where

$x_a$ —the width of the device (mm);

$x_b$ —minimum movement distance between individual devices and the support (mm);

$$H_{\min} = \left( \sum y_a + \sum y_b \right) \cdot 1.1 \text{ (mm)}, \quad (2)$$

where

$y_a$ —height of the device in a given cross-section (mm);

$y_b$ —minimum movement distance between the device and the support (mm).

Taking into account the dimensions of machines and devices and the movement distances (Table 2), the minimum width and height were calculated according to Equations (3) and (4).

$$S_{\min} = [(1350 + 1200 + 700 + 315) + (250 + 400)] \cdot 1.1 = 4640 \text{ mm} \quad (3)$$

$$H_{\min} = [(155 + 1500 + 500) + (300)] \cdot 1.1 = 2700 \text{ mm} \quad (4)$$

Then, based on the calculated values of  $S_{\min}$  and  $H_{\min}$ , the ŁP8/V29/A three-part support was selected [34] (Table 3), which should meet the conditions of Equations (5) and (6).

$$S_{\text{catalogue}} \geq S_{\min} \quad (5)$$

$$H_{\text{catalogue}} \geq H_{\min} \quad (6)$$

**Table 3.** Basic dimensions of the support arches ŁP8.

Type of Support	Height, $H_{\text{catalogue}}$ (mm)	Width, $S_{\text{catalogue}}$ (mm)	Cross-Section (m <sup>2</sup> )
ŁP7/V29/A	3100	4200	11.08
ŁP8/V29/A	3300	4700	13.07
ŁP9/V29/A	3500	5000	14.76

The three types of supports are presented in the Table 3 in order to show the optimal arch yielding support selection. The first type, ŁP7/V29/A, was not selected because it did not meet the  $S_{\text{min}}$  condition. However, the third type, ŁP9/V29/A, was also not selected due to the too high costs of roadway support; therefore, type ŁP8/V29/A was selected. Thus, the condition was met because  $4700 \text{ mm} \geq 4640 \text{ mm}$  and  $3300 \text{ mm} \geq 2700 \text{ mm}$ . The arrangement of machines and devices with spaces is shown in Figure 6.

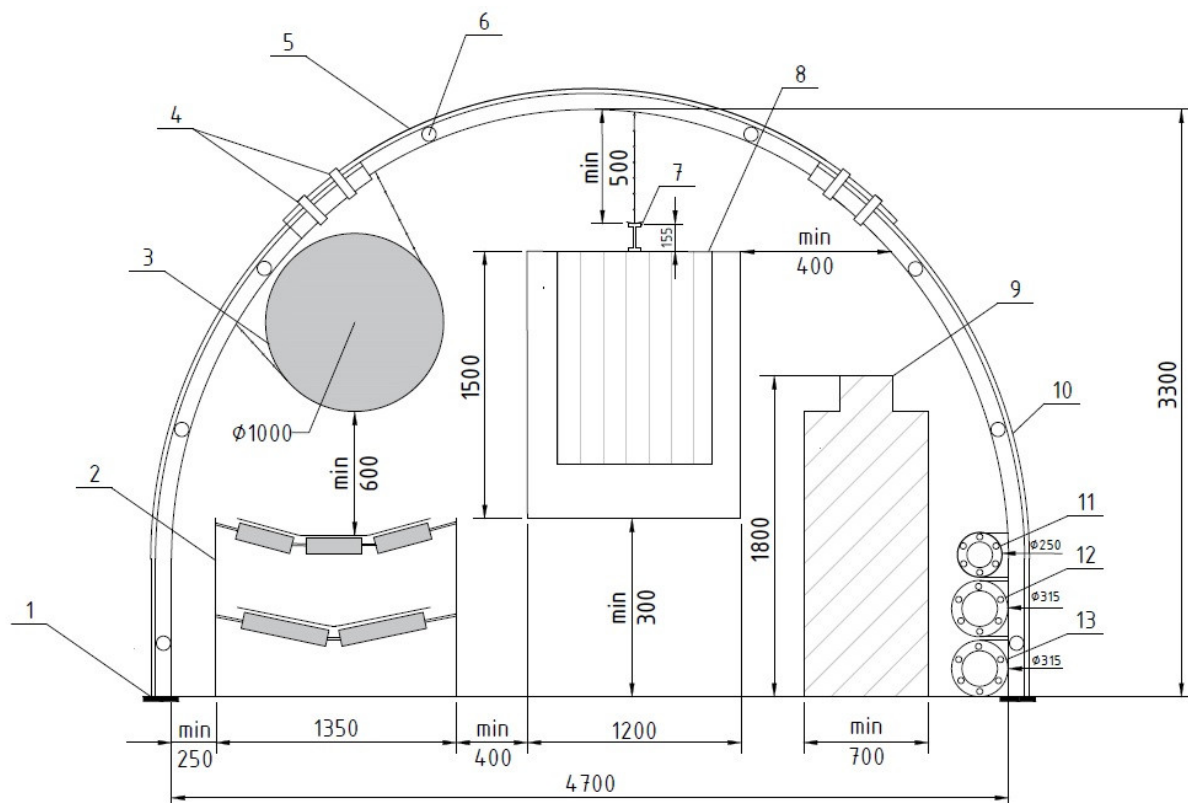


**Figure 6.** Cross-section of the roadway II: 1—support foot; 2—belt conveyor GWAREK-1000; 3—duct; 4—double yoke stirrups; 5—roof arch of the yielding support ŁP8/V29/A; 6—multi-element strut; 7—rail of suspended monorail; 8—BIZON 120-X suspended monorail; 9—passage for miners; 10—sidewall arch; 11—compressed air pipeline; 12—drainage pipeline; 13—fire pipeline.

The arch yielding support was made of steel elements with a “V” profile. As it is a preparatory excavation not exposed to the effects of longwall exploitation, no convergence was observed at the driving stage. The expected course of the slide of the steel sets elements at the longwall exploitation stage is estimated at the level of  $0.3 \text{ mm/m}$ . In order to define the dimensions of the roadway II cross-section in the breakout,  $300 \text{ mm}$  was added to the catalogue height and width. Therefore, the height  $H_w$  and width  $S_w$  of the excavation cross-section in the breakout were calculated according to Equations (7) and (8):

$$H_w = H_{\text{kat}} + 300 = 3600 \text{ mm}, \quad (7)$$

where

$H_w$ —height of the cross-section of the excavation in the breakout (mm);

$H_{kat}$ —catalogue height of the ŁP8 support arches ( $H_{catalogue} = 3300$  mm);

$$S_w = S_{kat} + 300 = 5000 \text{ mm}, \quad (8)$$

where:

$S_w$ —width of the cross-section of the excavation in the breakout (mm);

$S_{kat}$ —catalogue width of the ŁP8 support arches ( $S_{catalogue} = 4700$  mm).

### 3.2. Ventilation Criterion

The selected dimensions of the arch yielding support must meet the ventilation requirements for preparatory workings [35]. For this purpose, the actual velocity  $V_{rz}$  of the flowing air in the excavation was determined, and then the value was compared with the calculated values of the minimum  $V_{min}$  and maximum  $V_{max}$  velocity. For the designed roadway excavation, there must be the following relationship (9):

$$V_{min} \leq V_{rz} \leq V_{max} \left( \frac{m}{s} \right), \quad (9)$$

where

$V_{rz}$ —actual air flow velocity (m/s);

$V_{max}$ —permissible maximum air velocity in the excavation (m/s);

$V_{min}$ —the minimum permissible air velocity in the excavation (m/s).

The actual air flow velocity  $V_{rz}$  in the excavation was calculated according to Equation (10):

$$V_{rz} = \frac{Q_a}{F}, \left( \frac{m}{s} \right), \quad (10)$$

where

$Q_a$ —the required air flow rate at the outlet from the duct ( $m^3/s$ ) was calculated according to Equation (11) [36];

$F$ —usable cross-section of the excavation ( $m^2$ ), assumed  $F = 13.07$   $m^2$  (Table 3);

$$Q_a = \frac{Q_b}{P_q}, \left( \frac{m^3}{s} \right), \quad (11)$$

where

$Q_b$ —fan flow,  $m^3/s$  (for Axial Flow Fan—Type ES 9-500/80,  $Q_b = 10.2$   $m^3/s$ ) [37];

$P_q$ —the expenditure reserve ratio (dimensionless) is given by Equation (12):

$$P_q = 0.77 \cdot \exp \left( L \cdot \sqrt[3]{\frac{k^2}{2} \cdot r} \right) + 0.23 \cdot \exp \left( -2 \cdot L \cdot \sqrt[3]{\frac{k^2}{2} \cdot r} \right) \quad (12)$$

where

$L$ —length of the duct, m ( $L = 80$ );

$k$ —leakage rate of the duct,  $m^3/(sN^{1/2})$  ( $k = 0.003$ );

$r$ —unit resistance, flow rate of the duct,  $Ns^2/m^9$  ( $r = 0.003590$ ).

The actual air flow velocity  $V_{rz}$  was 4.87 m/s.

The minimum air velocity in excavation  $V_{min}$  is associated with the indication of whether the designed excavation is subject to the methane hazard. The air velocity in the excavation, which is ventilated by a duct in non-methane fields or in methane fields of I category methane hazard, cannot be less than 0.15 m/s, and in methane fields II, III and IV of the methane hazard category, it cannot be less than 0.3 m/s [35]. Roadway II is not covered by the methane hazard, so  $V_{min} = 0.15$  m/s. The maximum air velocity in the excavation  $V_{max}$  for the exploitation excavations cannot exceed 5 m/s, for the preparatory excavations 8 m/s, and in shafts and small shafts, it cannot exceed 12 m/s [35]. Due to the fact that roadway II is a preparatory excavation,  $V_{max} = 8$  m/s. After specifying the value

of the actual, minimum and maximum velocities, they were inserted into Equation (9), which shows that the ventilation criterion for the driven excavation was met because  $0.15 \leq 4.87 \leq 8$  m/s.

### 3.3. Arch Yielding Support Calculation

The arch yielding support for roadway II was selected according to the method of Professor Rułka [38]. It is one of the three methods commonly used in Polish underground hard coal mining. This method can be used if the weighted average value of the compressive strength of the indicated roof rock package is not less than 10 MPa; the weighted average water permeability value of the indicated roof and floor rock packages is at least 0.5; the energy of probable tremors in the vicinity of the designed excavation is not greater than  $5 \times 10^5$  J; the angle of the transverse inclination of the rock layers is not more than  $30^\circ$ ; the angle of the excavation is not more than  $35^\circ$ . In addition, the designed excavation is located at a depth of 300–1200 m and the width of the cross-section of the excavation in the breakout is a maximum of 8 m. In order to determine the geomechanical properties of rocks in the area of the designed excavation, the range of the  $Z_{\text{roof}}$  and  $Z_{\text{floor}}$  rocks should be determined according to Equations (13) and (14):

$$Z_{\text{roof}} = 1.0 \cdot H_c \quad (13)$$

$$Z_{\text{floor}} = 0.5 \cdot H_c \quad (14)$$

where

$H_c$ —height of the cross-section of roadway II in the breakout (m).

Figure 7 shows the lithological profile of the rock range, which was taken into account when selecting the support for roadway II.

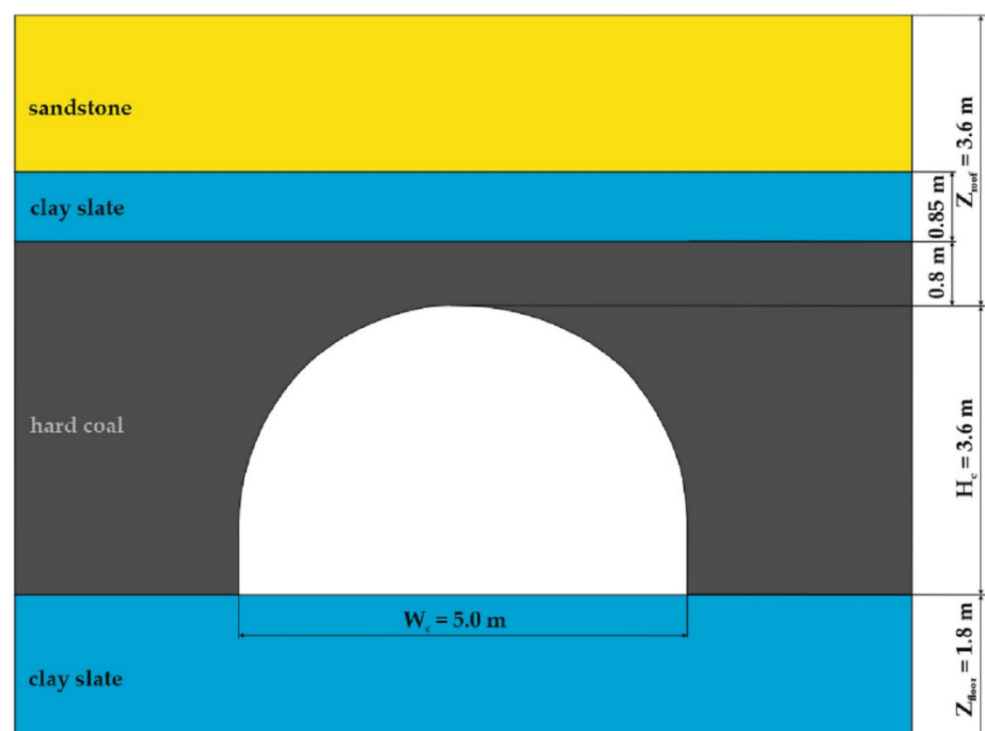


Figure 7. Lithological profile for roadway II.

The selection of the arch yielding support was calculated according to Equation (15):

$$d \leq \frac{W_{N_c}}{q_0} \quad (15)$$

where

$d$ —arch yielding support spacing, m;  
 $W_{Nc}$ —computational index of load capacity of support arches, MN/m;  
 $q_0$ —computational load, MPa.

The support load index  $W_{Nc} = 0.0905$  MPa was calculated according to Equation (16):

$$W_{Nc} = 0.5544 \cdot W_N \cdot 0.8 \cdot k_1 \quad (16)$$

where

$W_N$ —load capacity index of support arches, MN/m (for section V29 made of steel S480W,  $W_N = 0.255$ ) [39];

$k_1$ —lining coefficient (in the designed excavation a tight lining will be used; therefore  $k_1 = 0.8$ ; for mechanical, loose and non-loose lining, the coefficient is, respectively: 1.0, 0.6 and 0.4);

0.5544—constant value related to the factor of utilization of the maximum load capacity of arches;

0.8—constant value related to the load unevenness factor.

The computational load  $q_0 = 0.0357$  MPa is calculated according to Equation (17):

$$q_0 = k_g \cdot k_u \cdot k_\alpha \cdot k_\beta \cdot k_e \cdot k_s \cdot q_N + q_d, \text{ MPa}, \quad (17)$$

where

$k_g$ —the rock mass weakening coefficient in the determined rock packet (Figure 7), which ranges from 0.79 to 3.64,  $k_g = 1.881$ , was calculated according to Equation (18):

$$k_g = 1.7391 \cdot (1.1 - 0.007 \cdot RQD) \cdot (2.8 - 1.8 \cdot R_s) \cdot (1.07 - 0.0002 \cdot H), \quad (18)$$

where

$H$ —depth of roadway II,  $H = 800$  m;

$RQD$ —rock quality designation,  $RQD = 40\%$ ;

$R_s$ —coefficient of the influence of rock moisture on their strength,  $R_s = 0.75$ ;

$k_u$ —fault action coefficient for excavations that are located in the fault zone  $k_u = 1.2$ ;

$k_\alpha$ —coefficient of the influence of the transverse inclination of the rock layers, for  $\alpha \leq 15^\circ$ ;

$k_\alpha = 1.0$ , while for  $15^\circ \leq \alpha \leq 35^\circ$   $k_\alpha = 1.15$ ;

$k_\beta$ —coefficient of the longitudinal inclination of the excavation impact, for  $\beta \leq 15^\circ$   $k_\beta = 1.0$ , while for  $15^\circ \leq \beta \leq 25^\circ$   $k_\beta = 1.15$  and for  $25^\circ \leq \beta \leq 35^\circ$   $k_\beta = 1.20$ ;

$k_e$ —exploitation edge influence factor (roadway II is outside the impact range and a distance of more than 120 m from the edge, therefore  $k_e = 1$ );

$k_s$ —the impact factor of the adjacent excavation (roadway II is driven parallel to roadway I at a distance of about 225 m) according to Formula (19),  $k_s = 1.0$ :

$$k_s = 1 + \frac{1}{\left(1 + \frac{x_s}{W_c}\right)^2} \quad (19)$$

where

$W_c$ —width of the excavation in the breakout,  $W_c = 5$  m (Figure 7);

$x_s$ —distance between roadways,  $x_s = 225$  m (Figure 4);

$q_N$ —the characteristic value of the vertical static loads of the support,  $q_N = 0.0446$ , was calculated according to Equation (20):

$$q_N = q_w \cdot \frac{W_{ca}}{W_c}, \text{ MPa}, \quad (20)$$

where

$W_{ca}$ —computational width,  $W_{ca} = 7.1798$ , which is calculated according to Equation (21):

$$W_{ca} = W_c + H_c \cdot k_0, \text{ m}, \quad (21)$$

$W_c$ —width of the excavation in the breakout,  $W_c = 5$  m (Figure 7);

$H_c$ —height of the excavation in the breakout,  $H_c = 3.6$  m (Figure 7);

$k_0$ —coefficient of the influence of the angle of internal friction of rocks in the sidewall (compressive strength of coal = 15.45 MPa (Table 1),  $k_0 = 0.6055$ );

$q_w$ —conditional pressure. Taking into account the effect of depth, coal compression strength and design width),  $q_w = 0.0311$  MPa, was calculated according to Equation (22):

$$q_w = 0.001 \cdot (0.357 \cdot W_{ca} + 21.425) \cdot (0.0019 \cdot H + 0.4187) \cdot (1.145 - 0.0145 \cdot C_{sroof}), \text{ MPa}, \quad (22)$$

where

$W_{ca}$ —computational width, m;

$H$ —depth of roadway II,  $H = 800$  m;

$C_{sroof}$ —weighted average compressive strength of rocks in roof rocks (Table 1 and Figure 7),

$C_{sroof} = 32.7$  MPa;

$Q_d$ —dynamic unit load was determined on the basis of Figure 8,  $q_d = 0.015$  (roadway II is located 50 m below the shock layer, and the expected shock energy is  $1 \times 10^5$  J).

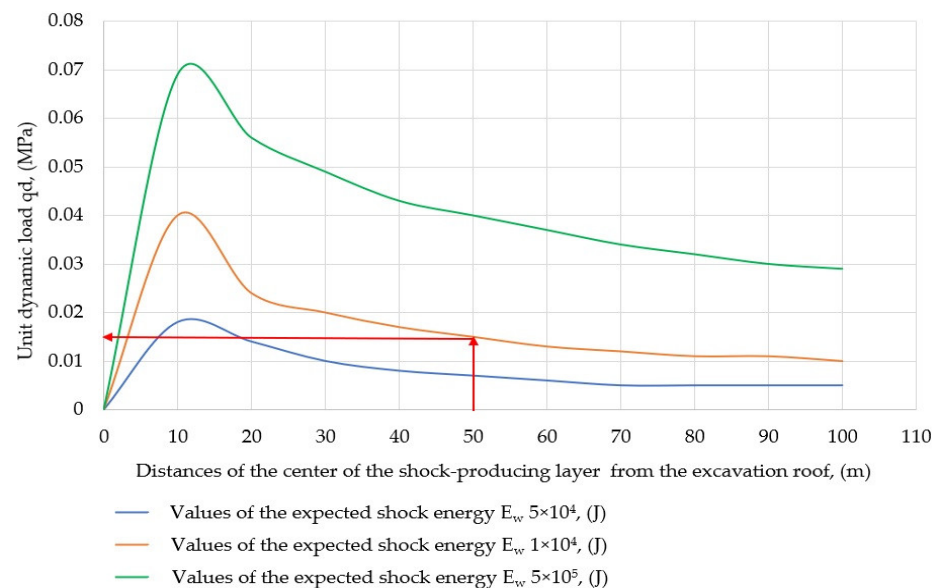


**Figure 8.** Dependence of the unit dynamic load  $q_d$  on the value of the expected shock energy  $E_w$  and the distance of the center of the shock-producing layer from the excavation roof.

After selecting all the coefficients, the support spacing was calculated according to Formula (15). The calculations were made for the part of the excavation without the fault (23) and with its impact (24).

$$d_{\text{without fault}} \leq \frac{W_{Nc}}{q_0} = \frac{0.0905}{0.098} = 0.92 \text{ m} \quad (23)$$

$$d_{\text{with fault}} \leq \frac{W_{Nc}}{q_0} = \frac{0.0905}{0.1156} = 0.78 \text{ m} \quad (24)$$

The calculations show that, for the part of the excavation without the fault, the support spacing should be less than 0.92 m. However, the impact contributes to the reduction in spacing to 0.78 m. Due to the geometry of the struts used to stabilize the support arches, it can be assumed that, in the fault zone, support spacing should be 0.75 m and 0.9 m outside of it.

#### 4. Discussion

Driving preparatory workings is a fundamental goal for the exploitation of a deposit with a longwall panel. For this reason, the optimization and continuous improvement

of the efficiency of driving and securing workings in the vicinity of faults are important issues. A thorough analysis of the geological conditions, taking into account the experience gained during the previous works in similar conditions, is the basis for making a decision on the possibility and method of securing the excavation while passing through the fault. While driving the preparatory workings, headgate and tailgate, their performance may be suspended as a result of discontinuous deformations. A special case is the situation when the excavation of the excavation does not reveal any significant geological disturbances that could affect production capacities and, in the course of further progress, one encounters obstacles such as thickness reduction and faults that prevent effective driving. This is an obvious financial loss of underground mining plants related to the expenditure on the construction of such workings. Due to the fact that, in Poland, the basic type of support for preparatory excavations is the arch yielding support, and only in two underground coal mines (“Bogdanka” and Budryk”) a separate rock bolt support was used in the research roadway, the article attempts to present the advantages of an independent bolt support, which can be an alternative to currently used security methods. Taking into account the rising prices of steel, limiting its consumption by introducing the bolt support can bring significant savings for the mining plant. Cost elements are closely related to labor, materials, equipment and transportation. One solution contributing to the reduction in overall costs may be to replace the arch yielding support with rock bolts, of course if the geological conditions allow the use of this type of support. In accordance with Polish mining regulations [35], the use of a separate rock bolt support in coal mining plants is allowed for preparatory and room workings with a cross-sectional area not exceeding 30 m<sup>2</sup> and a working width not exceeding 7 m. In addition, the roof rocks have an average-weighted uniaxial compressive strength, tested for a rock packet with a thickness of 3 m, that is not less than 15 MPa for layers with a plate structure and rock quality designation not less than 20% or 10 MPa for layers with a massive structure, and quality designation of not less than 40%. In addition, the rock mass is dry or non-sagging, and the water permeability coefficient is not less than 0.8. Currently, the rock bolt support is embedded in the carbon rock mass only by means of the resin cartridges and a cement binder. Expansion or friction bolts are not used. A threaded rod with a length of up to 2.7 m is made of a steel ribbed bar, while longer bolts are made as a cables or strings up to 15 m long. The calculation of the economic effects due to the use of a stand-alone rock bolt support consists in comparing the costs incurred for making the excavation in the bolted support with the costs incurred for making the same excavation in the arch yielding support (Table 4).

**Table 4.** Cost structure for arch yielding and rock bolt supports.

Cost	Arch Yielding Support with a Cross-Section of 13 m <sup>2</sup>	Rock Bolt Support in Length 2.5 m
Labour, %	19.51	37.78
Material, %	71.81	51.11
Equipment, %	3.25	6.67
Transport, %	5.42	4.44
Total cost of 1 m, PLN	3690	2250

The largest issue, accounting for more than half of the total cost of a stand-alone rock bolt support, is the materials. The costs of material, equipment and transport per meter of the excavation are relatively constant over a certain period of time, while the labor costs change with the increase in productivity, which in turn is conditioned by the increase in experience acquired by the mining crew and the use of highly efficient and failure-free equipment. Due to the compressive strength of coal, which in the area of the designed excavation is only 0.45 MPa higher (Table 1) above the minimum value, a decision was made not to use a separate bolt support. In order to determine the impact of the fault on the

change in the total displacement around the roadway, a spatial numerical model was built in the RS3 software [40] based on the finite element method. The main goal of numerical simulations was to determine the difference in changing the total displacement distribution for an excavation without support and that is secured by means of steel arch yielding without and with steel segments. The rock mass model was cubic with a side length of 60 m (Figure 9a–c). In the coal layer, an excavation 5 m wide and 3.6 high was designed.

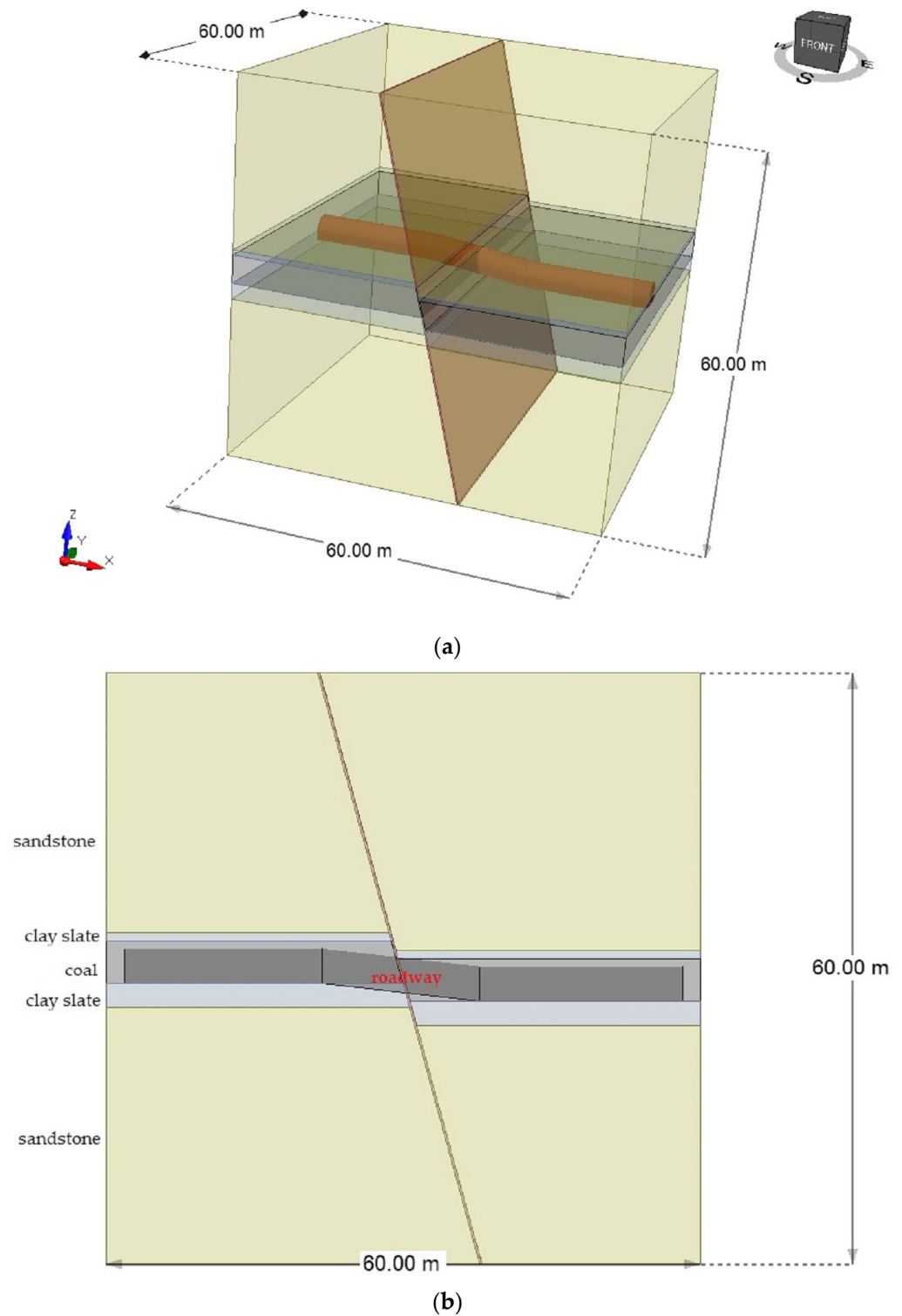
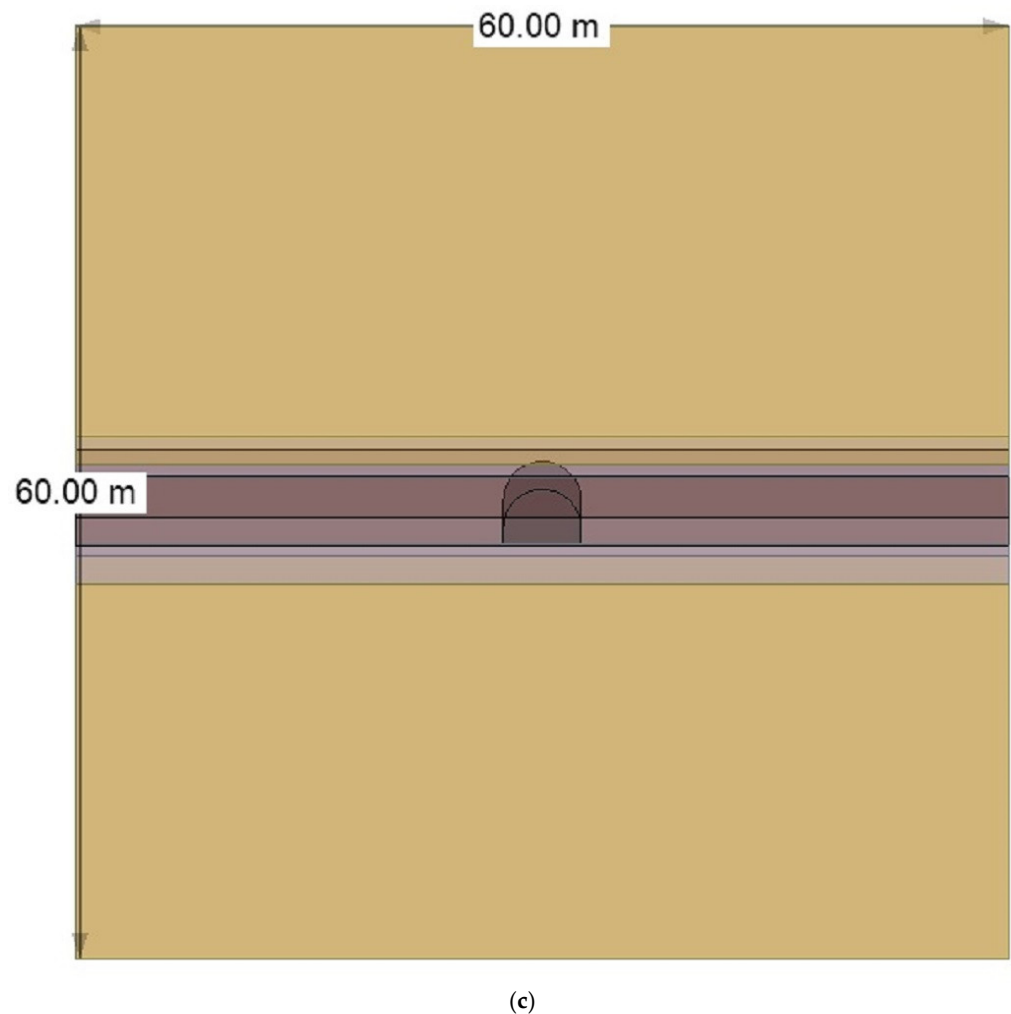


Figure 9. Cont.



**Figure 9.** Rock mass model: (a) spatial view; (b) side view; (c) front view.

The horizontal extent of the zone of increased impact of the rock mass on the support due to the fault on both sides of the fault plane was determined according to Equation (25) [38]:

$$L_u = \frac{2.5 \cdot \sqrt{h_u}}{\sin \delta} \quad (25)$$

where

$L_u$ —fault action zone (m);

$h_u$ —the height of the fault throw (m);

$\delta$ —the angle of the fault plane ( $^\circ$ ).

For a fault with the throw size  $h = 1.8$  m and the inclination angle of the fault plane  $\delta = 75^\circ$ ,  $L_u = 3.47$  m. Moreover, when the fault crosses the excavation (Figure 4), the fault zone of the fault  $L_u$  should be double. Therefore, in the numerical model, both in front of and behind the fault, the compaction zone of the arch yielding support was at least 7 m. Out of several dozen possibilities of failure criteria offered by the RS3 numerical program, the Generalized Hoek–Brown criterion was selected, which belongs to the elastic/plastic group. The material constants were adopted from RocData software [41]. The strength, deformation and structural parameters for the individual layers and for the fault are presented in Table 5. In the model, it was assumed that the width of the fault gap was 0.2 m and that it was filled with crushed rocks. The arch yielding support and steel straight segments were modeled as beam elements, for which the minimum tensile strength for the S480W steel grade is 480 MPa. The support spacing in the fault zone and outside

this zone was 0.75 m and 0.9 m, respectively. The results of the calculations are shown in Figure 10a–c.

**Table 5.** Geomechanical parameters adopted in the numerical models.

Type of Rock	Unit Weight (MN/m <sup>3</sup> )	Compressive Strength (MPa)	Young's Modulus (MPa)	Poisson Ratio	Geological Strength Index	m <sub>b</sub>	s	a
Coal	0.0127	15.45	2300	0.3	65	0.756	0.009	0.502
Claystone	0.0239	16.5	10,300	0.23	70	1.678	0.018	0.501
Sandstone	0.0251	47	5400	0.25	75	5.169	0.036	0.501
Fault	0.0127	12.36	2000	0.3	50	0.185	0.001	0.506

The maximum value of total displacement around the roadway without support was 0.02 m. This value occurs in the roof of the hanging part in the immediate vicinity of the fault. Securing the excavation with the arch yielding support at a spacing of 0.9 m and 0.75 m in the fault impact zone reduces the value of total displacements by 10%. On the other hand, the additional reinforcement of the support with steel segments causes the value of total displacements to drop to 0.016 m, which is 80% of the value for the excavation without the support.

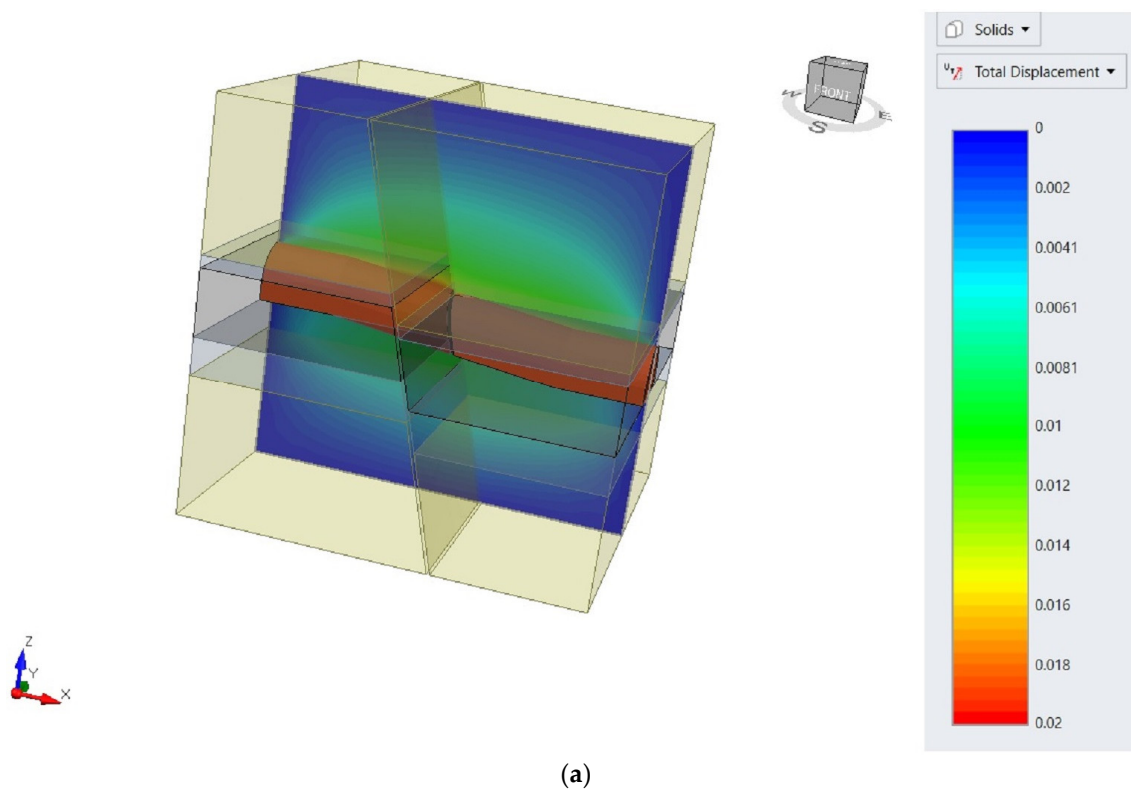


**Figure 10.** Cont.

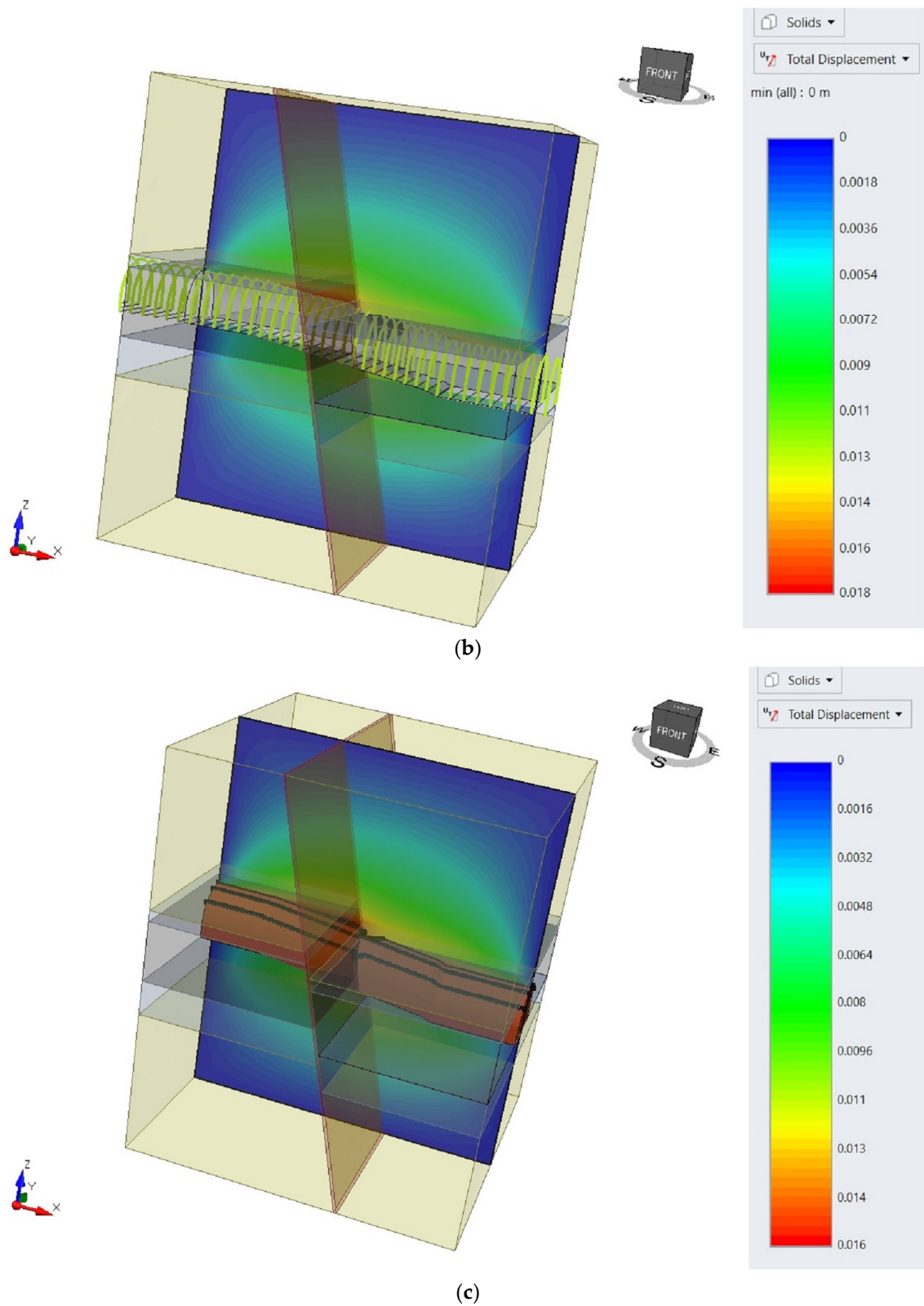


**Figure 10.** Total displacement distribution around the roadway: (a) without support; (b) with the arch yielding support; (c) with arch yielding and steel straight segments support.

## 5. Conclusions

In order to ensure the stability of the preparatory excavation, all possible negative factors affecting the mining and geological conditions of the excavation area should be

taken into account. As a result of the application of the minimum contours method, the ventilation criterion and geomechanical calculations, the ŁP8/V29 arch yielding supports with a spacing of 0.9 m were selected. If the excavation passes through a fault, the spacing was reduced to 0.75 m. The fault zone, both in front of and behind the fault, was calculated at 7 m. Based on numerical calculations, the following was found:

1. The projected total displacement around the roadway without support, which crosses the fault, was 0.02 m, while the use of the arch yielding support at a distance of 0.9 m outside the fault and 0.75 m in the fault zone reduces the total displacement value by 10%;
2. Additional reinforcement of the support in the form of steel straight segments contributes to a reduction in the value of total displacement by 11% and 20% compared to the excavation with and without the support.

The selection of driving roadways and mining supports in the fault conditions is associated with the necessity to use additional reinforcement and increasingly durable mining supports. In the case of support arches made of flexible arches, increasingly larger sizes of sections are used, which can be additionally made of steel with increased strength parameters. Due to the implementation of more and more modern mechanization of both transport and driving processes, the support of preparatory workings has increasingly larger cross-sectional dimensions. It is connected with the necessity to provide more and more working space for machines and devices, as well as for miners. Correctly selected support for preparatory workings is one of the most important issues when performing works in accordance with mining technology, because it plays a key role in ensuring the safety of the crew and continuity of production. The difficulty of designing the support increases with the deteriorating mining and geological conditions, such as the state of increased stress or discontinuous deformation of the rock mass. Although the method of securing workings in hard coal mines has not changed for several years, because preparatory workings mainly use the arch yielding support, all time activities are based on research and previous experience aimed at the most optimal selection of the support along with its strengthening in the given conditions of the rock mass. Strengthening the support of roadways in hard coal mines is a commonly used practice. The need to increase the load-bearing capacity of the used support occurs both at the stage of driving the excavation in the event of worse geological conditions, e.g., a fault, and during the operation of the excavation associated with an additional dynamic load. The experience and practice in the use of the support so far shows that, in most cases, the possible variants of increasing the load-bearing capacity of the support are not planned in advance, but their ad hoc methods are used, which have worked well in the given conditions earlier not necessarily taking into account the fact of whether the selected reinforcement variant for a given case is an optimal variant. However, the continuous possibility of modifying the load-bearing capacity of the casing is its undoubted advantage and the fact that it permits the obtainment of the expected effect, which is the smallest possible deformation of the support, allowing for the safety and full functionality of the excavation in accordance with the assumptions.

**Author Contributions:** Conceptualization, K.S. and K.Z.; methodology, K.S. and K.Z.; software, K.S.; validation, K.S., K.Z. and A.Z.; formal analysis, K.S., K.Z. and A.Z.; investigation, K.S., K.Z. and A.Z.; resources, K.S.; data curation, K.S., K.Z. and A.Z.; writing—original draft preparation, K.S.; writing—review and editing, K.S., K.Z., A.Z., D.B.A., J.W., H.X. and L.G.; visualization, K.S., K.Z. and A.Z.; supervision, K.S. and K.Z.; project administration, K.S.; funding acquisition, K.S. All authors have read and agreed to the published version of the manuscript.

**Funding:** This research was prepared as part of AGH University of Science and Technology in Poland, scientific subsidy under number: 16.16.100.215.

**Institutional Review Board Statement:** Not applicable.

**Informed Consent Statement:** Not applicable.

**Data Availability Statement:** The data presented in this study are new and have not been previously published.

**Conflicts of Interest:** The authors declare no conflict of interest.

## References

1. Cheng, G.; Li, L.; Zhu, W.; Yang, T.; Tang, C.; Zheng, Y.; Wang, Y. Microseismic investigation of mining-induced brittle fault activation in a Chinese coal mine. *Int. J. Rock Mech. Min. Sci.* **2019**, *123*, 104096. [CrossRef]
2. Burtan, Z.; Zorychta, A.; Cieřlik, J.; Chlebowski, D. Influence of mining operating conditions on fault behavior. *Arch. Min. Sci.* **2014**, *59*, 691–704. Available online: [https://journals.pan.pl/Content/93633/PDF/10267-Volume59\\_Issue3-08\\_paper.pdf?handler=pdf](https://journals.pan.pl/Content/93633/PDF/10267-Volume59_Issue3-08_paper.pdf?handler=pdf) (accessed on 20 November 2014). [CrossRef]
3. Li, Q.; Li, J.; Zhang, J.; Wang, C.; Fang, K.; Liu, L.; Wang, W. Numerical Simulation Analysis of New Steel Sets Used for Roadway Support in Coal Mines. *Metals* **2019**, *9*, 606. [CrossRef]
4. Xie, Z.; Zhang, N.; Wei, Q.; Wang, J.; Sharifzadeh, M. Study on Mechanical Properties and Application of a New Flexible Bolt. *Appl. Sci.* **2021**, *11*, 924. [CrossRef]
5. Wang, P.; Zhang, N.; Kan, J.; Wang, B.; Xu, X. Stabilization of Rock Roadway under Obliquely Straddle Working Face. *Energies* **2021**, *14*, 5759. [CrossRef]
6. Wang, J.; Apel, D.B.; Xu, H.; Wei, C.; Skrzypkowski, K. Evaluation of the Effects of Yielding Rockbolts on Controlling Self-Initiated Strainbursts: A Numerical Study. *Energies* **2022**, *15*, 2574. [CrossRef]
7. řrupárek, R.; Konečný, P. Stability of roadways in coalmines alias rock mechanics in practice. *J. Rock Mech. Geotech. Eng.* **2010**, *2*, 281–288. [CrossRef]
8. Shan, R.; Li, Z.; Wang, C.; Wei, Y.; Bai, Y.; Zhao, Y.; Tong, X. Research on the mechanism of asymmetric deformation and stability control of near-fault roadway under the influence of mining. *Eng. Fail. Anal.* **2021**, *127*, 105492. [CrossRef]
9. Mei, Y.; Li, W.; Yang, N.; Wang, G.; Li, T.; Sun, T. Failure Mechanism and Optimization of Arch-Bolt Composite Support for Underground Mining Tunnel. *Adv. Civ. Eng.* **2020**, *2020*, 5809385. [CrossRef]
10. Kang, H.; Jiang, P.; Wu, Y.; Gao, F. A combined “ground support-rock modification-destressing” strategy for 1000-m deep roadways in extreme squeezing ground condition. *Int. J. Rock Mech. Min. Sci.* **2021**, *142*, 104746. [CrossRef]
11. Liu, H.; Jiang, Z.; Chen, W.; Chen, F.; Ma, F.; Li, D.; Liu, Z.; Gao, H. A Simulation Experimental Study on the Advance Support Mechanism of a Roadway Used with the Longwall Coal Mining Method. *Energies* **2022**, *15*, 1366. [CrossRef]
12. Horst, R.; Modrzik, M.; Ficek, P.; Rotkegel, M.; Pytlik, A. Corroded steel support friction joint load capacity studies as found in Piast-Ziemowit coal mine. *Min. Inform. Autom. Electr. Eng.* **2018**, *1*, 81–94. [CrossRef]
13. Zhou, Q.; Herrera-Herbert, J.; Hidalgo, A. Predicting the Risk of Fault-Induced Water Inrush Using the Adaptive Neuro-Fuzzy Inference System. *Minerals* **2017**, *7*, 55. [CrossRef]
14. Cao, Z.; Gu, Q.; Huang, Z.; Fu, J. Risk assessment of fault water inrush during deep mining. *Int. J. Min. Sci. Technol.* **2022**, *32*, 423–434. [CrossRef]
15. Chen, J.; Dai, X.; Zhang, J. Analytical Study of the Confining Medium Diameter Impact on Load-Carrying Capacity of Rock Bolts. *Math. Probl. Eng.* **2021**, *2021*, 6680886. [CrossRef]
16. Qian, D.; Zhang, N.; Pan, D.; Xie, Z.; Shimada, H.; Wang, Y.; Zhang, C.; Zhang, N. Stability of Deep Underground Openings through Large Fault Zones in Argillaceous Rock. *Sustainability* **2017**, *9*, 2153. [CrossRef]
17. Kalmet. Available online: [https://www.kalmet.com.pl/pl/oferta/elementy\\_obudow\\_gornicznych.html](https://www.kalmet.com.pl/pl/oferta/elementy_obudow_gornicznych.html) (accessed on 19 February 2022).
18. Pytlik, A. Experimental studies of static and dynamic steel arch support load capacity and sliding joint temperature parameters during yielding. *Arch. Min. Sci.* **2020**, *65*, 469–491. [CrossRef]
19. Grodzicki, M.; Rotkegel, M. The concept of modification and analysis of the strength of steel roadway supports for coal mines in the Soma Basin in Turkey. *Studia Geotech. Mech.* **2018**, *40*, 38–45. [CrossRef]
20. HutaLab. Available online: <http://www.hutalab.com.pl> (accessed on 22 February 2022).
21. Rotkegel, M. ŁPw Steel Arch Support—Designing and Test Results. *J. Sustain. Min.* **2013**, *12*, 34–40. [CrossRef]
22. Li, W.; Liu, J.; Chen, L.; Zhong, Z.; Liu, Y. Roadway Support in Deep “Three-Soft” Coal Seam: A Case Study in Yili Mining Area, China. *Shock Vib.* **2021**, *2021*, 8851057. [CrossRef]
23. Yang, R.; Li, Q.; Li, Q.; Zhu, X. Assessment of Bearing Capacity and Stiffness in New Steel Sets Used for Roadway Support in Coal Mines. *Energies* **2017**, *10*, 1581. [CrossRef]
24. Lv, Z.; Qin, Q.; Jiang, B.; Luan, Y.; Yu, H. Comparative study on the mechanical mechanism of confined concrete supporting arches in underground engineering. *PLoS ONE* **2018**, *13*, e0191935. [CrossRef] [PubMed]
25. Wu, H.; Jia, Q.; Wang, W.; Zhang, N.; Zhao, Y. Experimental Test on Nonuniform Deformation in the Tilted Strata of a Deep Coal Mine. *Sustainability* **2021**, *13*, 13280. [CrossRef]
26. Wang, H.; Jiang, Y.; Xue, S.; Mao, L.; Lin, Z.; Deng, D.; Zhang, D. Influence of fault slip on mining-induced pressure and optimization of roadway support design in fault-influenced zone. *J. Rock Mech. Geotech. Eng.* **2016**, *8*, 660–671. [CrossRef]
27. Wang, H.; Shi, R.; Lu, C.; Jiang, Y.; Deng, D.; Zhang, D. Investigation of sudden faults instability induced by coal mining. *Saf. Sci.* **2019**, *115*, 256–264. [CrossRef]

28. Lu, Y.; Wei, W.; Zhiyu, T. Study on Mechanical Mechanism and Stability of Surrounding Rock in Fault Structure Roadway. *ResearchSquare* **2021**, *2*, 1–22. [[CrossRef](#)]
29. Adoko, A.C.; Yakubov, K.; Kaunda, R. Reliability Analysis of Rock Supports in Underground Mine Drifts: A Case Study. *Geotech. Geol. Eng.* **2021**, *11*, 2101–2116. [[CrossRef](#)]
30. Xiong, Y.; Kong, D.; Cheng, Z.; Wen, Z.; Ma, Z.; Wu, G.; Liu, Y. Instability Control of Roadway Surrounding Rock in Close-Distance Coal Seam Groups under Repeated Mining. *Energies* **2021**, *14*, 5193. [[CrossRef](#)]
31. Regulation of the Minister of the Environment of January 29, 2013 on Natural Hazards in Mining Plants. Natural Hazards in Mining Plants. Available online: <https://www.prawo.pl/akty/dz-u-2021-1617-t-j,17955795.html> (accessed on 10 February 2022). (In Polish).
32. Polish Standard: PN-93/G-04558. Hard Coal. Determination of Spontaneous Ignition Indexes. Polish Committee for Standardization: Warszawa, Poland, 1993. (In Polish)
33. Polish Standard: PN-G/06009. Horizontal and Inclined Underground Roadways in Mine Enterprises—Movement Clearances and Dimensions of Man Passages. Polish Committee for Standardization: Warszawa, Poland, 1997. (In Polish)
34. Polish Standard: PN-93/G-15000/02. Roadway Support with Susceptible Timber Frames Made of Special Sections. Arch Susceptible Frames LP of Sections Type V, Series A. Dimensions. Polish Committee for Standardization: Warszawa, Poland, 1993. (In Polish)
35. Tchórzewski, K. Regulation of the Minister of Energy on detailed requirements for the operation of underground mining plants of 23 November 2016. *J. Laws* **2017**, *1118*, 18. (In Polish)
36. Waclawik, J. *Mine Ventilation*; AGH Publishing House: Kraków, Poland, 2010; Volume I, p. 391. (In Polish)
37. CST. Available online: <https://cst-germany.com/pl/product/axial-flow-fan-type-es9-500-80-pu-stage-id184> (accessed on 24 February 2022).
38. Rułka, K.; Mateja, J.; Kowalski, E.; Skrzyński, K.; Stałęga, S.; Wojtusiak, A.; Schinohl, J. *Simplified Rules for the Selection of Frame Support for Roadway Workings in Hard Coal Mining Plants*; Central Mining Institute Publishing House: Katowice, Poland, 2001; pp. 1–30. (In Polish)
39. Polish Standard: PN-H-93441-1:2013-12. Hot Rolled Steel Sections for Mining-Part 1: General Requirements and Research. Polish Committee for Standardization: Warszawa, Poland, 2013. (In Polish)
40. RocScience. Available online: <https://www.rocsience.com/software/rs3> (accessed on 10 March 2022).
41. RocData. Available online: <https://www.rocsience.com/support/rocddata/release-notes> (accessed on 12 March 2022).